

DESY 95-124
hep-ph/9507271

Nonsinglet Contributions to the Structure Function g_1 at Small-x

J. Bartels

II. Institut für Theoretische Physik, Universität Hamburg

B.I.Ermolaev¹

A.F.Ioffe Physical-Technical Institute, St.Petersburg, 194021, Russia

M. G. Ryskin²

St.Petersburg Nuclear Physics Institute, Gatchina, St.Petersburg, 188350, Russia

Abstract: Nonsinglet contributions to the $g_1(x, Q^2)$ structure function are calculated in the double-logarithmic approximation of perturbative QCD in the region $x \ll 1$. Double logarithmic contributions of the type $(\alpha_s \ln^2(1/x))^k$ which are not included in the GLAP evolution equations are shown to give a stronger rise at small-x than the extrapolation of the GLAP expressions. Further enhancement in the small-x region is due to non-ladder Feynman graphs which in the DLA of the unpolarized structure functions do not contribute. Compared to the conventional GLAP method (where neither the whole kinematical region which gives the double logs nor the non-ladder graphs are taken into account) our results lead to a growth at small-x which, for HERA parameters, can be larger by up to factor of 10 or more.

¹The research described in this paper has been made possible in part by the Grant R2G 300 from the International Science Foundation and the Russian Government. This work has also been supported by the Volkswagen-Stiftung.

²Work supported by the Grant INTAS-93-0079 and by the Volkswagen-Stiftung

1 Introduction

In the framework of perturbative QCD the theoretical investigation of deep inelastic scattering in the HERA regime puts particular emphasis on the calculation of structure functions in the region $x \ll 1$. So far, main attention has been given to the small- x behavior of the gluon structure function: from the theoretical point of view, the strong rise predicted by perturbative QCD violates unitarity and hence requires corrections which restore unitarity. Experimentally, such a rise has been observed, and it is attractive to interpret it as a manifestation of the BFKL Pomeron [1].

From the theoretical side, however, also the fermion structure functions have quite an interesting small- x behaviour. Recently [2] it has been shown, for the case of the flavor nonsinglet contribution to F_1 , that the small- x behavior of quark structure functions is stronger than what one would obtain from simply extrapolating the GLAP [3, 4] evolution equations into the small- x region. The reason for this lies in the fact that at small- x a new region in phase space opens up which gives rise to logarithms of the type $(\alpha_s \ln^2(1/x))^n$ and which is not taken into account within the GLAP method. As long as we are dealing only with neutral currents and unpolarized structure functions, this observation may seem to be slightly academic, since the gluons in the flavor singlet will dominate at small x , and the quarks represent a nonleading effect. The situation, however, changes drastically if one considers, for example, polarized structure functions and their sum rules [5]. It is well known [4] that the polarized gluon structure function is no longer growing as $(1/x)^\lambda$ with λ close to 1, but rather with a λ close to 0. Consequently, the polarized gluons are no longer dominating over the fermions, and the small- x behavior of the quarks becomes as vital for polarized deep inelastic structure functions as that of the gluons.

It may be useful to briefly review the small- x behavior of the (unpolarized) gluon structure function in the GLAP scheme and in the BFKL Pomeron. As it is well known, GLAP sums logarithms of the type $(\alpha_s \ln(Q^2/\mu^2))^k$, whereas BFKL keeps terms of the form $(\alpha_s \ln(1/x))^k$. In the region of mutual overlap where the DLA is valid one is summing terms of the form $(\alpha_s \ln(Q^2/\mu^2) \ln(1/x))^k$. In terms of the anomalous dimension γ_{gg} of the two-gluon operator, the GLAP formalism uses a fixed order (one or two-loop) in α_s expression. As a function of n , $\gamma_{gg}(n)$ is singular near $n = 1$ (n is the moment index which in the small- x region coincides with angular momentum j of the cross channel). In contrast, the BFKL Pomeron provides all singular terms of the form $\sum(\alpha_s/(n-1))^k c_k$. Finally, in a physical gauge both GLAP and the BFKL Pomeron are sums of ladder diagrams, but the phase space for the transverse momenta of the gluons has, in the GLAP case, the property of strong ordering, whereas in the BFKL approximation this feature is almost completely lost ³.

This situation changes if we consider fermions at small x [2]. It has been observed almost 30 years ago [6] that in the Regge limit scattering amplitudes with two fermions

³During the rapidity evolution of the BFKL Pomeron, the mean value of the logarithm of the transverse momentum is still growing, but the fluctuations are much larger than in the GLAP case.

in the t-channel have two powers of $\ln(s/\mu^2)$ per loop, i.e. one is summing terms of the form $(\alpha \ln^2(s/\mu^2))^n$ rather than single logs. These double-logs cannot be reached within the GLAP scheme which, at small x , only includes the (less important) terms of the form $(\alpha_s \ln(Q^2/\mu^2) \ln(1/x))^n$. This difference is seen very clearly if one analyses the relevant region of integration inside the fermion ladders: GLAP has the same ordering of transverse momenta as in the gluon ladders, but the double-logs [6] come from a region with no ordering in k_T or the angle θ . Only the longitudinal components of the Sudakov variables are still ordered. In other words, in addition to the GLAP region there is another part of the phase space which contributes to these double-logs. Finally, it is instructive to describe this difference also in terms of the anomalous dimension. Within the GLAP analysis the anomalous dimension of the quarks, as a function of the moment index $n \approx j$, has a pole near $n=0$. In the Regge analysis which includes the double-logs, one obtains a quite different dependence upon n ; only for $\sqrt{\alpha_s} \ll n \ll 1$ one recovers the usual result. The small- x behavior, on the other hand probes the region $n \sim \sqrt{\alpha_s}$, where the two methods lead to different predictions.

In this paper we will calculate the small- x behavior of the nonsinglet contribution to the polarized structure function g_1 ; in a forthcoming paper we will extend our analysis to the flavor singlet part which contains mixing between the quarks and the gluons. We find that the small- x behavior is stronger than the extrapolation of the GLAP formula predicts. In comparison with the fermions in the unpolarized structure function [2] the polarized quark structure functions have another new property. In contrast to F_1 where a simple ladder structure gave the relevant logarithms, the polarized structure function g_1 receives contributions also from non-ladder graphs. Our analysis will show that these terms lead to a further enhancement at small- x .

This paper is organized as follows. In section 2 we briefly review the definitions of the structure functions, and we discuss their signature properties by studying the double logarithmic contributions of the first two loop corrections. In section 3 we construct the infrared evolution equation for g_1 and find its solution. The final section 4 contains a brief discussion of our results.

2 Signatures of the Structure Functions

The standard parametrization of the hadron tensor $W_{\mu\nu}$ of deep inelastic scattering (neglecting the contribution of weak currents) has the form [7]:

$$W_{\mu\nu} = \left(-g_{\mu\nu} + \frac{q_\mu q_\nu}{q^2}\right)F_1 + \left(p_\mu - q_\mu \frac{pq}{q^2}\right)\left(p_\nu - q_\nu \frac{pq}{q^2}\right)\frac{F_2}{pq} + \iota\epsilon_{\mu\nu\alpha\beta}q^\alpha s^\beta \frac{m}{pq}g_1 + \iota\epsilon_{\mu\nu\alpha\beta}q^\alpha (s^\beta - p^\beta \frac{sq}{pq})\frac{m}{pq}g_2 \quad (2.1)$$

where p, s, m are the four momenta of the incoming parton (quark), its polarization vector and its mass, resp., and q the lepton momentum transfer ($-q^2 = Q^2$). The structure functions F_1, F_2, g_1 , and g_2 depend upon Q^2 and $x = Q^2/2pq$.

The structure functions in (1) are energy discontinuities of scattering amplitudes for the elastic Compton scattering of a virtual photon off the proton. In analogy with (1) we write:

$$\begin{aligned}
T_{\mu\nu} &= \imath \int d^4x e^{\imath qx} \langle N | T(J_\mu(x) J_\nu(0)) | N \rangle \\
&= (-g_{\mu\nu} + \frac{q_\mu q_\nu}{q^2}) T_1 + (p_\mu - q_\mu \frac{pq}{q^2})(p_\nu - q_\nu \frac{pq}{q^2}) T_2 \\
&\quad + \imath \epsilon_{\mu\nu\alpha\beta} q^\alpha s^\beta \frac{m}{pq} T_3 + \imath \epsilon_{\mu\nu\alpha\beta} q^\alpha (s^\beta(pq) - p^\beta(sq)) \frac{m}{pq} T_4
\end{aligned} \tag{2.2}$$

with

$$F_1 = -\frac{1}{2\pi} \text{Im} T_1 \quad F_2 = -\frac{pq}{2\pi} \text{Im} T_2 \tag{2.3}$$

$$g_1 = -\frac{1}{2\pi} \text{Im} T_3 \quad g_2 = -\frac{pq}{2\pi} \text{Im} T_4 \tag{2.4}$$

It is easy to see that these amplitudes satisfy the following crossing symmetry relations: T_1, T_2 and T_4 are symmetric with respect to the replacement $s \rightarrow -s$ (i.e. $s \rightarrow u$ channel), while the amplitude T_3 changes sign. Indeed, the tensor $T_{\mu\nu}$ is symmetric under the interchange of μ and ν and $q \rightarrow -q$. But $q \rightarrow -q$ means $x \rightarrow -x$, i.e. $s \rightarrow u$. Since the tensors in front of T_1 and T_2 are symmetric, T_1 and T_2 must be even under $s \rightarrow u$. Correspondingly, T_3 must be odd, and T_4 whose tensor has an additional power of q , is even again. In other words, T_1, T_2, T_4 are the amplitudes of the positive signature, and T_3 has the negative signature.⁴ In the following we shall concentrate on this odd signature case T_3 which gives g_1 .

One can check the main implications of the signature assignment by simply calculating the amplitudes in lowest order perturbation theory. In the Born approximation they take the form:

$$T_1^{(0)} = e_q^2 \left(\frac{s}{s - Q^2 + \imath\epsilon} + \frac{-s}{-s - Q^2 + \imath\epsilon} \right), \tag{2.5}$$

$$T_2^{(0)} = e_q^2 \frac{4Q^2}{s^2} \left(\frac{s}{s - Q^2 + \imath\epsilon} + \frac{-s}{-s - Q^2 + \imath\epsilon} \right), \tag{2.6}$$

$$T_3^{(0)} = e_q^2 \left(\frac{s}{s - Q^2 + \imath\epsilon} - \frac{-s}{-s - Q^2 + \imath\epsilon} \right), \tag{2.7}$$

$$T_4^{(0)} = 0 \tag{2.8}$$

(e_q is the electric charge of the initial quark of flavour q .) We have deliberately chosen this particular way of writing eqs.(5-8) in order to stress that T_1 and T_2 are symmetric under the

⁴All the other kinematical factors (like pq) which sometimes enter into the definition of the structure functions do not change the signature (i.e. crossing symmetry) properties of a given amplitude.

replacement $s \rightarrow -s$, and T_3 is antisymmetric.

Now let us consider the radiative corrections to the T_i . In the one-loop approximation there are two Feynman graphs yielding DL-contributions to T_i (see Fig.2). However, since ultimately we are interested in the discontinuity of the amplitude, we have to consider, besides the DL-terms, also the $\imath\pi$ -parts of the energy logarithms. When $s > 0$, only the graph 2a yields the $\imath\pi$ -contribution. The result is:

$$T_1^{(1)} = e_q^2 \frac{g^2 C_F}{16\pi^2} \left[\ln^2\left(\frac{-s}{\mu^2}\right) + \ln^2\frac{s}{\mu^2} - 2\ln^2\frac{Q^2}{\mu^2} \right], \quad (2.9)$$

$$T_2^{(1)} = 2x T_1^{(1)}, \quad (2.10)$$

$$T_3^{(1)} = e_q^2 \frac{g^2 C_F}{16\pi^2} \left[\ln^2\left(\frac{-s}{\mu^2}\right) - \ln^2\frac{s}{\mu^2} \right], \quad (2.11)$$

$$T_4^{(1)} = 0 \quad (2.12)$$

where $C_F = (N^2 - 1)/2N$ for the colour group $SU(N)$, g is the QCD-coupling constant which we will keep fixed within the DLA, and μ is an infrared mass scale for the transverse momentum:

$$\mu < k_t \quad (2.13)$$

Eqs.(9-11) show that the one-loop expressions, $T_i^{(1)}$, for the functions T_i still have the same signatures as the Born terms. As a result, in T_1 and T_2 the double logs add up, whereas in T_3 only a term $\sim \imath\pi \ln(s/\mu^2)$ survives. For the energy discontinuity, in both T_1 and T_3 the $\imath\pi$ pieces in $\ln^2(s/\mu^2)$ give the relevant contribution. This pattern will not change if we include more rungs in higher orders in g^2 , i.e. when building the usual sum of ladder diagrams.

However, non-ladder Feynman diagrams can also contribute to T_i in the DLA, and their role is quite different for the even- and odd-signature amplitudes. For example, from the case of the elastic scattering of quarks it is known [8] that non-ladder graphs contribute differently to positive and negative signature amplitudes. In our case, the non-ladder diagrams first appear (within the DLA) in the two loop approximation, i.e. in the order g^4 of perturbation theory. They are illustrated in Fig.3. Let us study these contributions in more detail. In particular we want to demonstrate and explain that they do contribute to T_3 but not to T_1 or T_2 .

Following the line of arguments introduced in [6], each of the non-ladder diagrams can be viewed as being obtained from a ladder graph by adding non-ladder virtual gluons to it. In order to give the double logarithm, these gluons couple only to the side lines of the ladder (i.e. not to the rungs), and they must be softer (i.e. have smaller k_t) than all those ladder gluon rungs which are embraced by the non-ladder gluon. Otherwise they would destroy double logs of the ladder. Moreover, those propagators of the ladder to which the non-ladder gluon is attached, must be close to the mass shell - its virtuality should be smaller than the

transvers momentum square of the non-ladder gluon. In the following, these non-ladder type gluons will be called bremsstrahlung gluons. The important consequence of their “softness” is that, in the numerator of the expression for the non-ladder graph, the momenta of the bremsstrahlung gluons can be neglected compared to the ladder gluon momenta. Furthermore, the momenta along the side lines of the ladder, are small in comparison with the initial momenta q and p . In Fig.3 the momentum of the bremsstrahlung gluon is denoted by k_2 . The remaining momenta in all these numerators give, for each diagram, the factor $\pm 4k_1^2 \cdot pk_1$ (where the sign plus stands for the diagrams in Fig.3a,b, while the minus sign belongs to Figs.3c,d). In front of this numerator we have a tensor which is built from p_μ , q_μ or $g_{\mu\nu}$. These tensors are identical for the graphs (a,b,c,d), and those of the (a',b',c',d')-diagrams differ by the replacement $\mu \rightleftharpoons \nu$ and $q \rightarrow -q$.

The way in which these double logs sum up or cancel, depends upon color and signature. First it is easy to see that for a color singlet t-channel different bremsstrahlung gluons cancel: for example, in Fig.3a and c the bremsstrahlung gluons are emitted from the lower left external line, and we are summing over different end points. Since we have color zero in the t-channel, both contributions cancel. As a result, in this order all double log bremsstrahlung contributions in Fig.3 cancel (this will change when we go to higher order, as we shall discuss further below).

Signature becomes crucial when we consider the $i\pi$ terms which are essential for the s-discontinuity. To be more precise, starting from the order g^4 where the nonladder graphs appear, even and odd signature amplitudes start to behave quite differently. For example, the graphs in Figs.3a' and b' have no s-cuts, but those in c' and d' can be redrawn as shown in Fig.4, and therefore they contribute to the s-discontinuity. Combining Figs.3a,b with c',d' one finds cancellation for even signature, non-cancellation for odd signature. As a result, the non-ladder graphs contribute to T_3 , but not T_1 or T_2 . This is in accordance with the conclusion of [8] for the quark scattering amplitude.

When we move on to higher orders in g^2 , most of these features can easily be generalized. For the remainder of this section we remove the photon lines at the upper end, and we restrict ourselves to quark scattering. First let us return to the bremsstrahlungs gluons. Starting from a fermion ladder with a few gluon rungs, each non-ladder gluon will comprise a subset of the rungs. In order to give the maximal number of double logarithms, this bremsstahlung gluon must be softer (i.e. have smaller k_t) than any line of this subset of rungs; at the same time, the fermion lines to which the bremsstrahlung gluon couples must be softer than the gluon itself. This implies that the bremsstrahlung gluons form a “nested” structure. The summation of all these graphs is done as described in [8]. Consider a typical diagram; pick the internal line with the lowest k_t . If it is a fermion line, the amplitude can be decomposed as indicated in Fig.5a. If, on the other hand, it is a gluon line, it must be a bremsstrahlungs gluon which - according to Gribov’s theorem - [9] must go from one external leg to another (Fig.5b). The sum of all diagrams, therefore, can be written as shown in Fig.5c; the first term on the rhs denotes the Born term. If we take the derivative with respect to the infrared

cutoff μ^2 (which appears only in the line with the smallest momentum), then we arrive at the infrared evolution equation illustrated in Fig.5c (whether or not the Born term contributes to this derivative has to be decided from case to case). This is the infrared evolution equation which has proven to be an efficient instrument for the investigation of the elastic scattering of quarks [8], and also in inelastic reactions at high energies [10].

The presence of the second term on the rhs has an important consequence. Even we restrict ourselves to amplitudes with color zero in the t-channel, the colored gluon forces the four quark amplitude to be in a color octet. Therefore, this second part appears as an inhomogeneous term in the nonlinear evolution equation, and we have to solve a separate evolution equation for the color octet amplitude. Furthermore, in the case of a colour singlet amplitude this term contributes only to the odd signature, as it can be seen as follows. Consider, for example, the two diagrams shown in Fig.6a and b. For the odd-signature amplitude, they both come with the opposite sign. Redraw the first diagram as illustrated in Fig.6c, and note that the upper line to which the soft gluon couples has the opposite direction: this gives an additional minus sign from the color factor, and the two diagrams sum up. Conversely, in the even signature case they cancel. As a result, the nonplanar diagrams appear only in the odd signature amplitude.

Finally, the infrared evolution equation for the (even signature) octet amplitude. Following the same arguments as before, we are led to the nonlinear evolution equation whose structure we illustrate in Fig.7. In the second term, only the even signature color octet contributes: the gluon has negative signature, and for the subamplitude the even signature configuration gives the maximal number of double logs. Combining this with the color factors, one finds that only the color octet survives.

3 Infrared Evolution Equation for g_1

In this section we apply the methods outlined in the previous section in order to construct and solve the infrared evolution equation for the nonsinglet contribution to g_1 . We will take into account both the DL-contributions and the $i\pi$ contributions.

Let us consider, again, the forward elastic photon-quark scattering amplitude $T_{\mu\nu}$ in DLA. As before, q and p are the (collinear) four momenta of the photon and the quark, resp., and we are in the regime where $s \gg -q^2 = Q^2 \gg p^2$. The structure of the infrared evolution equation for quark scattering has been discussed in the previous section, and we now apply the same ideas to photon quark scattering. The equation is illustrated in Fig.8, and its origin is easily understood. The upper blob on the rhs denotes the photon-quark scattering amplitude with the lower (incoming) legs having transverse momentum square equal to the infrared cutoff μ^2 . The lower blob on the rhs represents a quark quark elastic scattering amplitude with $k_T^2 = \mu^2$ for all external momenta. In order to translate this into an explicit equation, we note that $T_{\mu\nu}$ depends upon the two variables $z = \ln(s/\mu^2)$ and $y = \ln(Q^2/\mu^2)$.

Therefore, the lhs of Fig.5 has the two terms:

$$-\mu^2 \frac{\partial T_{\mu\nu}}{\partial \mu^2} = \frac{\partial T_{\mu\nu}}{\partial z} + \frac{\partial T_{\mu\nu}}{\partial y}. \quad (3.1)$$

The convolution on the rhs becomes simpler if we write our amplitudes in the Mellin representation w.r.t. s ($z = \ln(s/\mu^2)$):

$$T_i(z, y) = \int_{-i\infty}^{i\infty} \frac{d\omega}{2\pi i} \left(\frac{s}{\mu^2}\right)^\omega \xi^{(i)} R_i(\omega, y), \quad (3.2)$$

where ω denotes the angular momentum j , and ξ is the signature factor:

$$\xi^{(i)} = \frac{e^{-i\pi\omega} + \tau_i}{2} \quad (3.3)$$

with $\tau_3 = -1$. As usual, the integration contour runs to the right of all singularities in the ω -plane. A similar representation is used for the quark-quark scattering amplitude, and the transform is denoted by $f_0^{(-)}$. The infrared evolution equation of Fig.8 then takes the form:

$$\omega R_i + \frac{\partial R_i}{\partial y} = \frac{1}{8\pi^2} R_i f_0^{(+)} \quad (3.4)$$

for $i=1,2$ and

$$\omega R_3 + \frac{\partial R_3}{\partial y} = \frac{1}{8\pi^2} R_3 f_0^{(-)} \quad (3.5)$$

for the amplitude T_3 . Eq.(3.4) has been discussed and solved in [2].

In order to solve eq.(3.5) for R_3 , we need to know $f_0^{(-)}$. This is the quark scattering amplitude discussed in the previous section. It satisfies the evolution equation of Fig.5 [8]:

$$f_0^{(-)}(\omega) = \frac{N^2 - 1}{2N} \frac{g^2}{\omega} - \frac{N^2 - 1}{N} \frac{g^2}{4\pi^2} \frac{1}{\omega^2} f_8^{(+)}(\omega) + \frac{1}{8\pi^2 \omega} \left(f_0^{(-)}(\omega)\right)^2 \quad (3.6)$$

The second term on the rhs is due to the signature changing contributions of gluon bremsstrahlung which lead us to define an even-signature quark quark scattering amplitude $f_8^{(+)}(\omega)$ with color octet quantum number in the t-channel. This amplitude has the infrared evolution equation shown in Fig.7:

$$f_8^{(+)}(\omega) = -\frac{g^2}{2N\omega} + \frac{Ng^2}{8\pi^2\omega} \frac{d}{d\omega} f_8^{(+)}(\omega) + \frac{1}{8\pi^2\omega} \left(f_8^{(+)}(\omega)\right)^2 \quad (3.7)$$

Its solution follows from the discussion given in [8]: using the transformation

$$f_8^{(-)}(\omega) = Ng^2 \frac{\partial}{\partial \omega} \ln u(\omega) \quad (3.8)$$

the Riccati equation (3.7) is equivalent to the linear differential equation

$$\frac{du^2}{dz^2} - z \frac{du}{dz} - \frac{1}{2N^2}u = 0 \quad (3.9)$$

where

$$z = \omega/\omega_0, \quad \omega_0 = \sqrt{Ng^2/8\pi^2}. \quad (3.10)$$

After a trivial transformation this equation is solved by a parabolic cylinder function. As a result, $f_8^{(+)}$ has the form:

$$\begin{aligned} f_8^{(+)}(\omega) &= Ng^2 \frac{d}{d\omega} \ln \left(e^{z^2/4} D_p(z) \right) \\ &= Ng^2 \frac{d}{d\omega} \ln \left(\int_0^\infty dt t^{-1-p} e^{-zt-t^2/2} \right) \end{aligned} \quad (3.11)$$

with

$$p = -1/2N^2. \quad (3.12)$$

With this we return to (3.6) and obtain for $f_0^{(-)}$:

$$f_0^{(-)} = 4\pi^2 \omega \left(1 - \sqrt{1 - \frac{g^2(N^2 - 1)}{4\pi^2 N \omega^2} [1 - \frac{1}{2\pi^2 \omega} f_8^{(+)}(\omega)]} \right) \quad (3.13)$$

(the minus sign in front of the square root follows from the requirement that, for large ω , the solution has to match the Born approximation).

Having found the function $f_0^{(-)}(\omega)$, we are now able to solve eq.(3.5):

$$R_3(\omega, y) = C(\omega) e^{(-\omega + f_0^{(-)}(\omega)/8\pi^2)y} \quad (3.14)$$

with some unknown function $C(\omega)$. This function is determined if we impose the matching condition [2]:

$$T_3(z, y=0) = \tilde{T}_3(z) \quad (3.15)$$

where $\tilde{T}_3(z)$ is the corresponding invariant amplitude with a (nearly) on-shell photon: $-q^2 = \mu^2$. Since this amplitude no longer depends upon Q^2 , its infrared evolution equation (which is the analogue of eq.(3.5))) has no y -derivative. On the other hand, its Born term now has a dependence upon μ^2 which is no longer negligible and leads to a nonzero contribution on the rhs (Fig.8). Denoting the Mellin transform of \tilde{T}_3 by \tilde{R}_3 the matching condition (3.15) simply becomes $C(\omega) = \tilde{R}_3$, and the equation for \tilde{R}_3 reads:

$$\omega \tilde{R}_3 = c_3 + \frac{1}{8\pi^2} \tilde{R}_3 f_0^{(-)}. \quad (3.16)$$

The boundary condition for \tilde{T}_3 is:

$$\tilde{T}_3(z=0) = \tilde{T}_{3\text{Born}} = c_3$$

$$\tilde{R}_3 = \frac{c_3}{\omega} \quad (3.17)$$

where $\tilde{T}_{3\text{Born}}$ is given in (2.7) and leads to $c_3 = 2e_q^2$.

Inserting the solution for $\tilde{R}_3 = C(\omega)$ into (3.15) we obtain:

$$T_3(z, y) = 2e_q^2 \int_{i\infty}^{i\infty} \frac{d\omega}{2\pi i} \left(\frac{s}{Q^2} \right)^\omega \xi^{(-)} \frac{1}{\omega - f_0^{(-)}(\omega)/8\pi^2} e^{yf_0^{(-)}(\omega)/8\pi^2} \quad (3.18)$$

In order to obtain our final result, g_1 , we have to take the discontinuity in s . With the signature factor $\xi^{(-)} = i\pi\omega/2$ and the variables $x = Q^2/s$ and Q^2 we arrive at

$$g_1(x, Q^2) = \frac{e_q^2}{2} \int_{-i\infty}^{i\infty} \frac{d\omega}{2\pi i} x^{-\omega} \left(\frac{Q^2}{\mu^2} \right)^{f_0^{(-)}(\omega)/8\pi^2} \frac{\omega}{\omega - f_0^{(-)}(\omega)/8\pi^2} \quad (3.19)$$

In the limit where $1/x$ is much larger than Q^2/μ^2 , the leading contribution comes from the rightmost singularity in the ω -plane.

4 Discussion

The most interesting aspect of our result (3.19) is the small- x behaviour. The leading singularity in the ω -plane is the branch point due to the vanishing of the square root in $f_0^{(-)}$ in (3.13). As a first approximation, let us take the number of colours N to be large. As it has been discussed in [8], $f_8^{(+)}$ can then be approximated by the first term on the rhs of (3.7) (i.e. its Born term), and the location of the branch point follows from the condition:

$$0 = 1 - \frac{g^2 N}{4\pi^2 \omega^2} \left[1 + \frac{g^2}{4\pi^2 N \omega^2} \right] \quad (4.1)$$

(note that our $\omega = j$, i.e. it differs from the $\omega = j-1$ which is commonly used in the context of the BFKL Pomeron and the unpolarized gluon structure function). Expanding in inverse powers of N we find for the first two terms:

$$\omega = \omega^{(-)} = \omega^{(+)} \left(1 + \frac{1}{2N^2} \right) \quad (4.2)$$

where

$$\omega^{(+)} = \sqrt{\frac{g^2(N^2 - 1)}{4N\pi^2}} \quad (4.3)$$

is the rightmost singularity for the flavor nonsinglet part of F_1 found in [2]. Let us stress that the leading singularity of the negative signature amplitude (g_1) is shifted to the right compared to the positive signature one $\omega^{(+)}$ [8]. Firstly such a behaviour of the negative signature amplitudes were noticed in [11] for the elastic scattering in QED.

A more accurate determination of the branch point singularity leads, instead of (4.2), to:

$$\begin{aligned}\omega^{(-)} &\approx \omega^{(+)} \cdot 1.04 \\ &\approx 0.41\end{aligned}\tag{4.4}$$

for $\alpha_s = 0.18$. As a result, the power of $1/x$ of the nonsinglet piece of g_1 is stronger than that of F_1 by about 4 %. This enhancement has its origin in the non-ladder graphs which were absent in the calculation of F_1 . In the HERA region, the enhancement of g_1 relative to F_1 [2] is approximately

$$\begin{aligned}g_1/F_1 &\approx 1. + \omega^{(+)} 0.04 [\ln(1/x) + \frac{1}{2} \ln(Q^2/\mu^2)] \\ &\approx 1.13\end{aligned}\tag{4.5}$$

for $x = 10^{-3}$, $Q^2 = 20 \text{GeV}^2$, and $\mu^2 = 4 \text{GeV}^2$. This estimate may serve as a crude method of estimating the non-singlet $g_1^{n.s.}$ in the small-x region, once $F_1^{n.s.}$ has been measured.

Let us finally see how our result (3.19) is related to the GLAP expression. To this end we take Q^2/μ^2 to be much larger than $1/x$; the exponent $f_0^{(-)}(\omega)/8\pi^2$ plays the role of the anomalous dimension γ_{qq} . For $\sqrt{\alpha_s} \ll \omega \ll 1$ (i.e. g^2/ω^2 is small) we obtain from (3.13):

$$\gamma_{qq}(\omega) = 2 \frac{\alpha_s}{4\pi\omega} \frac{N^2 - 1}{2N}\tag{4.6}$$

which agrees with the singular part of the quark anomalous dimension. In a straightforward extrapolation of the GLAP approximation into the small-x region [12, 13, 14] one would use this singular term in the anomalous dimension and performe a saddle point analysis. This has lead to the conclusion that at small x $g_1 \sim \exp(\sqrt{\text{const} \ln(Q^2/\Lambda^2) \ln(1/x)})$, in analogy with the small-x behavior of the gluon structure function (at fixed α_s). In contrast to this, our result in (3.19) gives a quite different answer for the ω dependence of the quark anomalous dimension and hence for the small-x behavior of g_1 . For a numerical estimate of the difference we simply combine (4.5) with the result for F_1 which was obtained in [2] (note that for the flavor nonsinglet case the γ_{qq} is the same for the polarized and the unpolarized structure function): for the non-singlet quark structure function with the initial condition $q(x, Q_0^2) \propto \delta(1 - x)$ ⁵ a comparison has been made of the GLAP-evolution at small-x and the double logarithmic formula derived in [2], and a difference of up to a factor of 10 (at typical HERA values for x and Q^2) was found. Together with (4.5), this leads to a slightly stronger discrepancy in g_1 : a factor of ten or even more.

⁵It does not seem very plausible to assume that $g_1(x, Q_0^2)$ is singular at $x \rightarrow 0$, therefore we think that the somewhat oversimplified δ -function ansatz is justified.

An even stronger discrepancy exists between our result and the Regge prediction [15, 16, 17]. For the flavor nonsinglet (isotriplet) exchange the small- x behavior is given by a_1 exchange. It has the form $(1/x)^{\alpha_R}$, and the a_1 intercept α_R is believed to lie somewhere between -0.5 and 0 [16], i.e. the flavor nonsinglet part of g_1 is predicted to be regular as $x \rightarrow 0$!

Having found that the double logarithms in the small- x region are numerically important, we have to address the slightly more involved analysis of the flavor singlet case. Here we are facing the mixing between gluons and quarks: as it can be seen from [4] or, more directly, from [12, 17], the small- x behavior of the polarized gluon structure function is less singular than the unpolarized one and, therefore, competes with the quarks. This analysis is in progress, and results will be presented in a forthcoming paper.

Acknowledgements: We are grateful to E.A.Kuraev, M.M Terekhov, and, especially, to L.N.Lipatov for useful discussions. Two of us (B.E. and M.R.) wish thank DESY for their hospitality.

Figure Captions:

Fig.1: The Born approximation for $T_{\mu\nu}$.

Fig.2: The one-loop approximation for $T_{\mu\nu}$.

Fig.3: Lowest order non-ladder gluons in $T_{\mu\nu}$.

Fig.4: The right hand cut energy discontinuities of the diagrams Figs.3a, b, and c': in the even signature amplitude, a and c' cancel (similary a and d', which is not shown in Fig.4), whereas in the odd signature case they are coming with the same sign and add up.

Fig.5: The line with lowest k_t in a general non-ladder diagram for the quark quark scattering amplitude, (a) a quark line, (b) a gluon line. (c) the infrared evolution equation for the sum of all non-ladder diagrams. The sum in front of the second term on the rhs denotes the different possibilities of attaching bremsstrahlung gluons to the external lines.

Fig.6: Cancellation of bremsstrahlung gluons in the even signature amplitude.

Fig.7: The infrared evolution equation for the octet even signature quark quark scattering amplitude. The sum in front of the second term on the rhs denotes the different possibilites ways of attaching bremsstrahlungs gluons to the external lines.

Fig.8: The infrared evolution equation for the photon quark scattering amplitude. The lower blob on the rhs denotes the quark quark scattering amplitude from Fig.5c.

References

- [1] E.A.Kuraev and L.N.Lipatov, V.S.Fadin, *Sov.Phys.JETP* **44** (1976) 443, *Sov.Phys.JETP* **45** (1977) 199,
Y.Y.Balitskij and L.N.Lipatov, *Sov.J.Nucl.Phys* **28** (1978) 822.
- [2] B.I.Ermolaev, S.I.Manayenkov, M.G.Ryskin, DESY-95-017.
- [3] V.N.Gribov and L.N.Lipatov, *Sov.Journ.Nucl.Phys.* **15**, 438 and 675 (1972).
Yu.L.Dokshitser, *Sov.Phys.JETP* **46** (1977) 641.
- [4] G.Altarelli and G.Parisi, *Nucl.Phys.B* **126**, 297(1977).
- [5] For a recent review see, for example: M.Anselmino, A.V.Efremov, and E.Leader, CERN-TH.7216/94 and to be published in *Physics Reports*.

- [6] V.N.Gribov, V.G.Gorshkov, G.V.Frolov, L.N.Lipatov, *Sov.J.Nucl.Phys.* **6** (1967) 95.
V.G.Gorshkov, *Sov.Phys.Yspeki* **16** (1973) 322.
- [7] B.L.Ioffe, V.A.Khoze, L.N.Lipatov, “Hard Processes“, Noth-Holland, Amsterdam, 1984,
- [8] R.Kirschner and L.N.Lipatov, *Nucl.Phys.* **B 213** (1983) 122.
- [9] V.N.Gribov, *Sov.J.Nucl.Phys.* **5** (1967) 280; B.I.Ermolaev, V.S.Fadin, L.N.Lipatov, *Sov.J.Nucl.Phys.* **45** (1985) 508.
- [10] B.I.Ermolaev and L.N.Lipatov, *Int.J.Mod.Phys.* **A4** (1989) 3147.
- [11] V.G.Gorshkov, L.N.Lipatov, L.N.Nesterov, *Yad.Fiz.* **9** (1969) 1221.
- [12] M.B.Einhorn and J.Soffer, *Nucl.Phys.* **B 274** (1986) 714.
- [13] R.D.Ball, S.Forte, G.Ridolfi, CERN-TH-95-31
- [14] F.Close and R.G.Roberts, *Phys.Lett.* **B 316** (1993) 165 and *Phys.Lett.* **B 336** (1994) 257.
- [15] R.L.Heimann, *Nucl.Phys.* **B 64** (1973) 429.
- [16] J.Ellis, M.Karliner, *Phys.Lett.* **B 213** (1988) 73.
- [17] S.D.Bass and P.V.Landshoff, *Phys.Lett.* **B 336** (1994) 537.

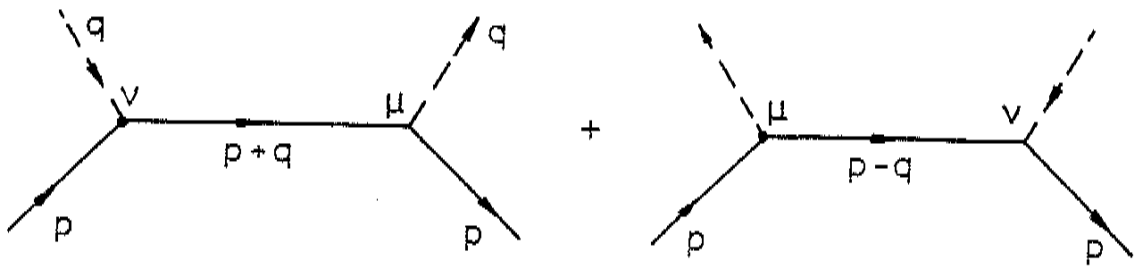
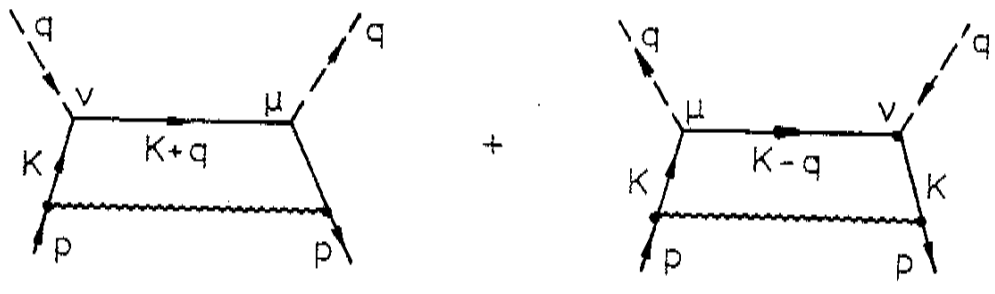


Fig.1



a

b

Fig.2

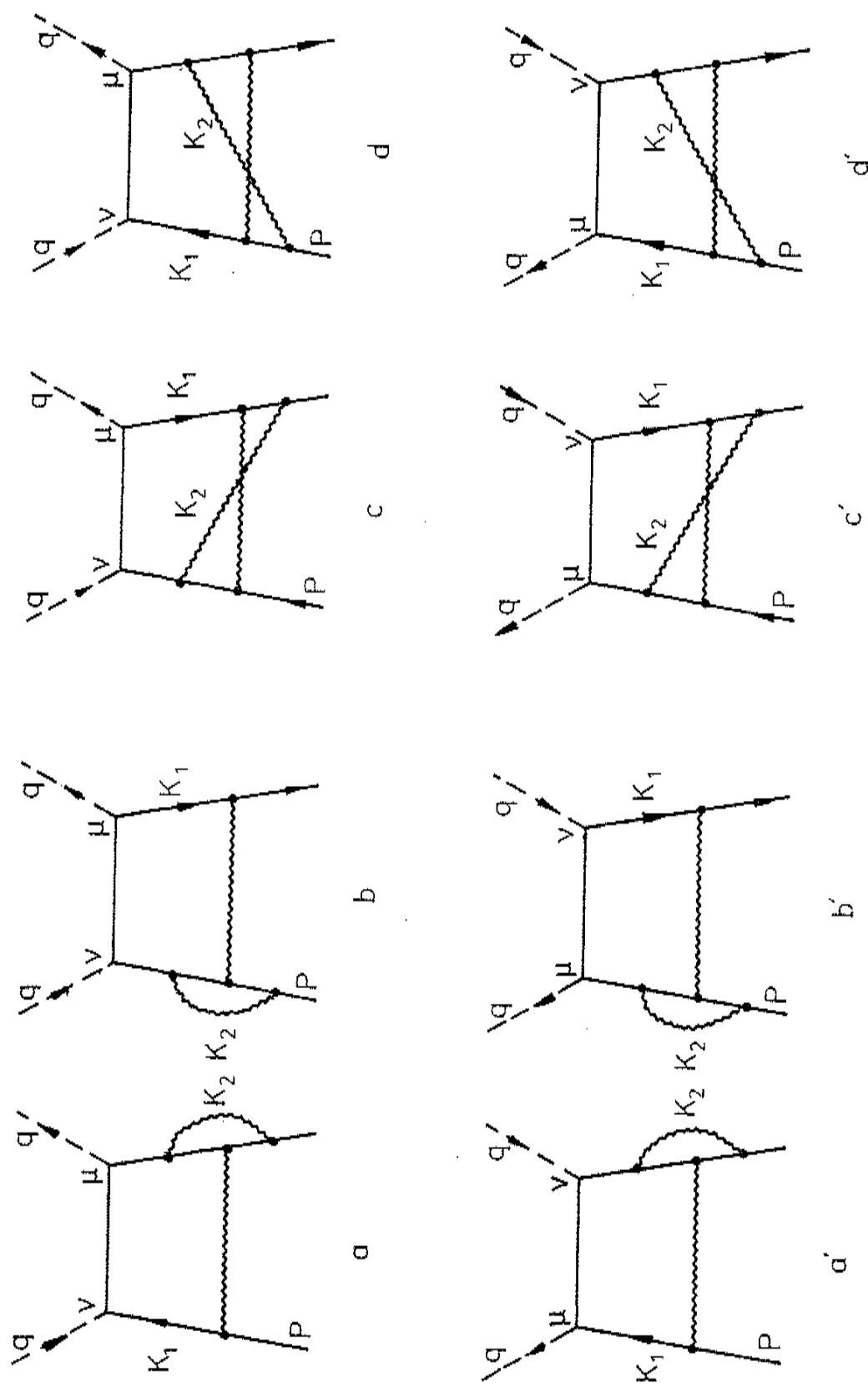


Fig. 3

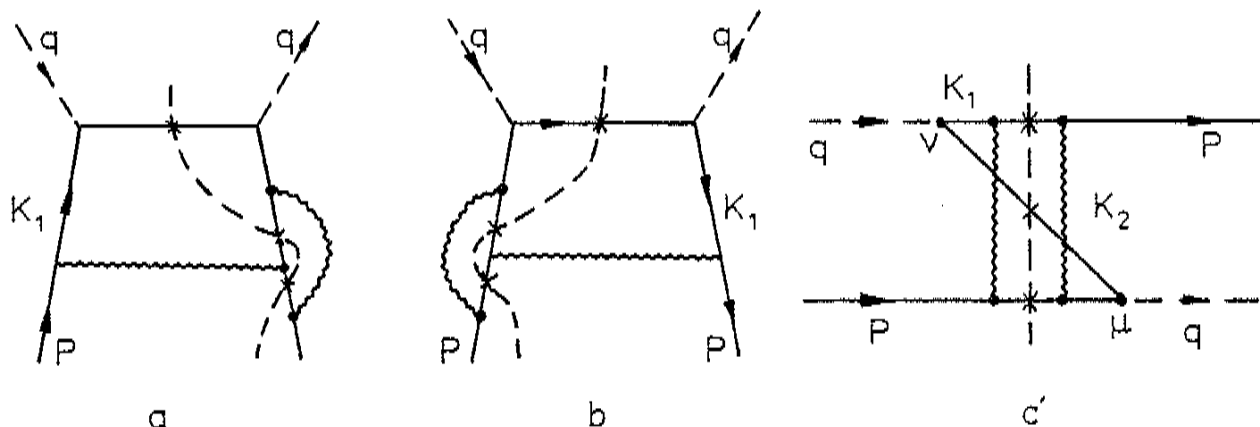
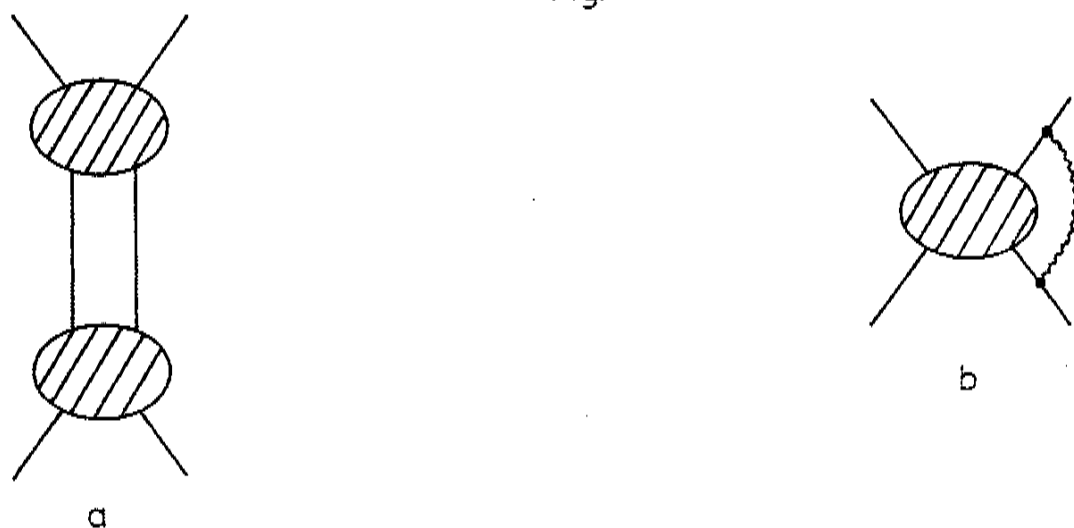


Fig. 4



$$\mu^2 \frac{\partial}{\partial \mu^2} \text{Diagram 0} = \mu^2 \frac{\partial}{\partial \mu^2} \text{Diagram A} + \mu^2 \frac{\partial}{\partial \mu^2} \sum \text{Diagram 8} + \mu^2 \frac{\partial}{\partial \mu^2} \text{Diagram B}$$

Fig. 5

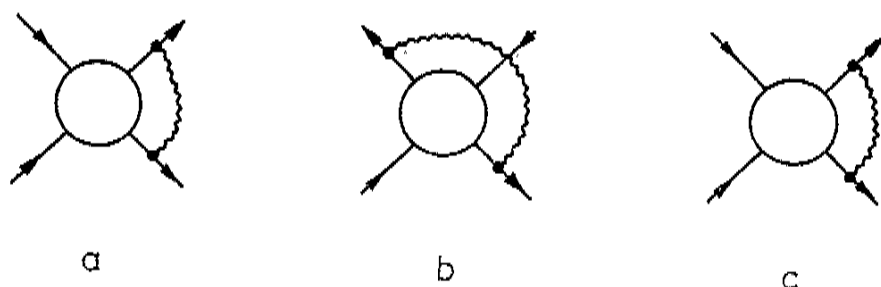


Fig. 6

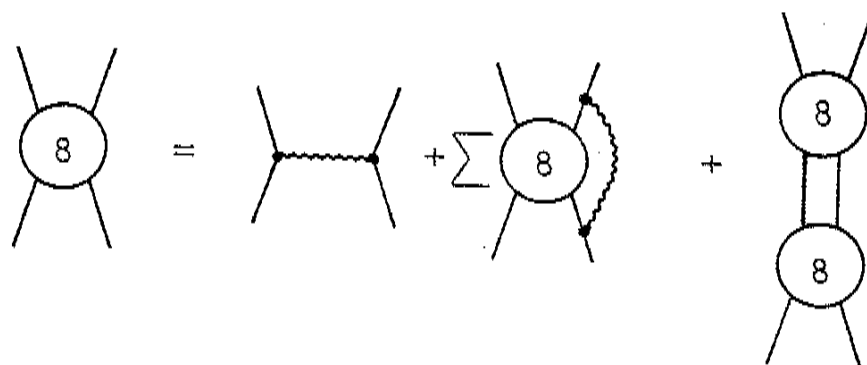


Fig. 7

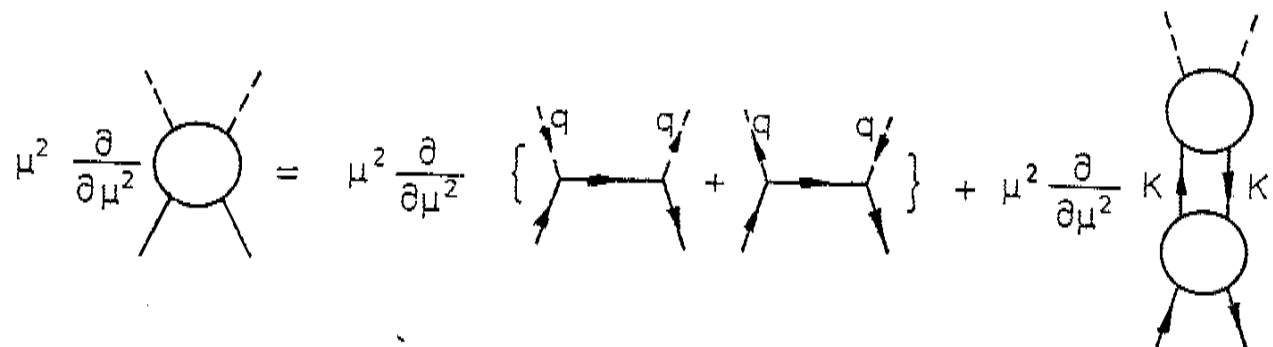


Fig. 8